Physica A 388 (2009) 3931–3938

Contents lists available at ScienceDirect

Physica A

journal homepage: www.elsevier.com/locate/physa

Assigning on-ramp flows to maximize highway capacity

Qiao-Ming Wang [a], Rui Jiang [b], Xiao-Yan Sun [a], Bing-Hong Wang [a,c,*]

[a] Department of Modern Physics, University of Science and Technology of China, Hefei 230026, People's Republic of China

[b] School of Engineering Science, University of Science and Technology of China, Hefei 230026, People's Republic of China

[c] The Research Center for Complex System Science, University of Shanghai for Science and Technology, Shanghai 200093, People's Republic of China

ARTICLE INFO

Article history:
Received 4 February 2009
Received in revised form 3 April 2009
Available online 29 May 2009

PACS:
45.70.Vn
89.75.-k
02.60.Cb

Keywords:
Traffic flow
NS model
Multiple on-ramps
Spatio-temporal patterns

ABSTRACT

In this paper, we study the capacity of a highway with two on-ramps by using a cellular automata traffic flow model. We investigate how to improve the system capacity by assigning traffic flow to the two ramps. The system phase diagram is presented and different regions are classified. It is shown that in region I, in which both ramps are in free flow and the main road upstream of the ramps is in congestion, assigning a higher proportion of the demand to the upstream on-ramp could improve the overall flow, which is consistent with previous studies. This is explained through studying the spatiotemporal patterns and analytical investigations. In contrast, optimal assignment has not been observed in other regions. We point out that our result is robust and model independent under certain conditions.

1. Introduction

Traffic congestion causes a huge waste of time and fuel as well as serious pollution all over the world. On highways, congestion is usually induced by various kinds of bottleneck, such as on-ramps, off-ramps, lane closures, speed limits, etc., among which the on-ramp is of particular interest and has been widely studied. For example, a capacity drop is widely observed when traffic flow transits from free flow to congested flow upstream of the on-ramps.

To enhance the capacity of a highway with an on-ramp, various kinds of method have been proposed. For example, the ramp metering method has been widely studied and applied in real traffic [1–6]. Recently, cooperative merge strategies have been investigated by Davis [7–9] and Jiang and Wu [10]. Jiang et al. have proposed to use a loop structure at the merge region of the on-ramp, and they show from simulations that the capacity could be increased [10]. Jiang et al. also proposed a special design of the merge section, i.e., to split the main road into several branches and then merge the branches together [11]. It is demonstrated that with the help of traffic light control, the inhomogeneous traffic is homogenized. Accordingly, the capacity increases.

Nevertheless, there usually exists more than one isolated on-ramp on real highways. One typical example is traffic corridors widely existing in the USA; see for example Fig. 1 in Ref. [12]. As Kerner and Klenov pointed out [13], interaction between the successive bottlenecks has a nontrivial influence on traffic flow, and thus needs to be investigated in details.

This paper considers one typical scenario of successive bottlenecks, i.e., a highway with two on-ramps. We study how to improve the system capacity by assigning traffic flow to the two ramps. A similar scenario has been studied before. For example, it is shown in the work of Zhang and Recker [12] that downstream ramps should be metered more persistently

* Corresponding address: Department of Modern Physics, University of Science and Technology of China, Hefei 230026.
E-mail address: bhwang@ustc.edu.cn (B.-H. Wang).

0378-4371/$ – see front matter © 2009 Elsevier B.V. All rights reserved.
doi:10.1016/j.physa.2009.05.030

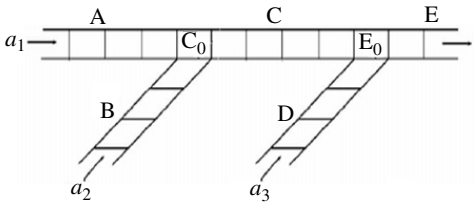

Fig. 1. Sketch of the two-on-ramp system.

than upstream ramps. A similar conclusion is drawn by Davis [14]: he pointed out that assigning a higher proportion of the demand to the upstream on-ramp could improve the overall flow. However, unfortunately, the reason why this result happens was not explored. Pica Ciamarra [15] carried out a more detailed study on this problem. Nevertheless, as indicated by the author, the on-ramps are modeled in a way of insertion probability, which is not realistic.

In this paper, we study the scenario by using the deterministic Nagel–Schreckenberg (NaSch) model [16]. We point out that our result is robust and model independent, provided the feature shown in Fig. 3 could be reproduced in the model. In our work, the interaction between on-ramps and the main road has been taken into account. Through studying the spatiotemporal patterns and analytical investigations, we have explained why the capacity could be improved by assigning a higher proportion of the demand to the upstream on-ramp. We also present the system phase diagram at different main road flow rates.

The paper is organized as follows. In Section 2, the model is briefly introduced. Section 3 presents and discusses the simulation results at different main road flow rates. The conclusion is given in Section 4.

2. Model

Fig. 1 shows the scenario of one highway with two on-ramps. For simplicity, the main road and the ramps are supposed to have only one lane. It is assumed that the two on-ramps connect to the main road at only one cell, C_0 and E_0, respectively. We denote the main road upstream of C_0, the first on-ramp, the main road between C_0 and E_0, the second on-ramp and the main road downstream of E_0 as roads A, B, C, D and E, respectively.

In our model, the cars move according to the deterministic NaSch model on the main road and on-ramps. Note that the result is robust and model independent; see Section 3. The parallel update rules of the deterministic NaSch model are as follows:

($R1$) acceleration: if $v_n < v_{\max}$, then $v_n \longrightarrow v_n + 1$;
($R2$) braking: if $v_n > d_n$, then $v_n \longrightarrow d_n$;
($R3$) motion: $x_n \longrightarrow x_n + v_n$.

Here v and x are the velocity and position of car n, respectively, $d = x_n + 1 - x_{n-1}$ is the spatial gap of car n, and $v_{\max}$ is the maximum velocity of cars. The road is divided into cells of length 7.5 m, and each car occupies one cell. One time step corresponds to 1 s and the maximum velocity is set to $v_{\max} = 5$.

We denote the leading cars on roads A, B, C, D as A_{lead}, B_{lead}, C_{lead}, D_{lead}, and the last cars on road C and E as C_{last} and E_{last}, respectively.

$$t_a = \frac{x_{C_0} - x_{A_{lead}}}{\min(v_{\max}, x_{C_{last}} - x_{A_{lead}} - 1, v_{A_{lead}} + 1)} \tag{1}$$

$$t_b = \frac{x_{C_0} - x_{B_{lead}}}{\min(v_{\max}, x_{C_{last}} - x_{B_{lead}} - 1, v_{B_{lead}} + 1)} \tag{2}$$

$$t_c = \frac{x_{E_0} - x_{C_{lead}}}{\min(v_{\max}, x_{E_{last}} - x_{C_{lead}} - 1, v_{C_{lead}} + 1)} \tag{3}$$

$$t_d = \frac{x_{E_0} - x_{D_{lead}}}{\min(v_{\max}, x_{E_{last}} - x_{D_{lead}} - 1, v_{D_{lead}} + 1)}. \tag{4}$$

We calculate the time needed to arrive at C_0 for cars A_{lead} and B_{lead} and at E_0 for cars C_{lead} and D_{lead}, expressed as t_a and t_b, t_c and t_d respectively, and update these cars as described by Ref. [17]. Specifically, for cars A_{lead} and B_{lead}, in one time step, the values of t_a and t_b are compared first. If $t_a > 1$ or $t_b > 1$, the updates of cars on road A and road B are not affected by each other; otherwise, i.e. $t_a \leq 1$ and $t_b \leq 1$, four cases are distinguished: (i), when $t_a < t_b$, car A_{lead} has the priority to occupy or pass lattice C_0, and become the new last car on road C, while the new velocity of car B_{lead} will be limited by the position of this new last car on road C; see Ref. [18]; (ii), when $t_a > t_b$, the situation is similar except for the exchange of roles of A_{lead} and B_{lead}; (iii), when $t_a = t_b$, for cars A_{lead} and B_{lead} with different distances to lattice C_0, the one nearer to C_0 is provided with priority to occupy or pass C_0 first, followed by the evolution of another one; (iv), when $t_a = t_b$ and cars A_{lead} and B_{lead} have the same distances to lattice C_0, car A_{lead} has the priority to update first because it is on the main road, and

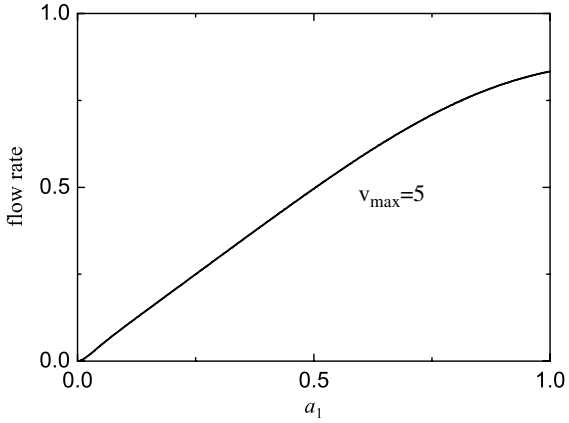

Fig. 2. The flow rate on the main road in the case when $a_2 = a_3 = 0$.

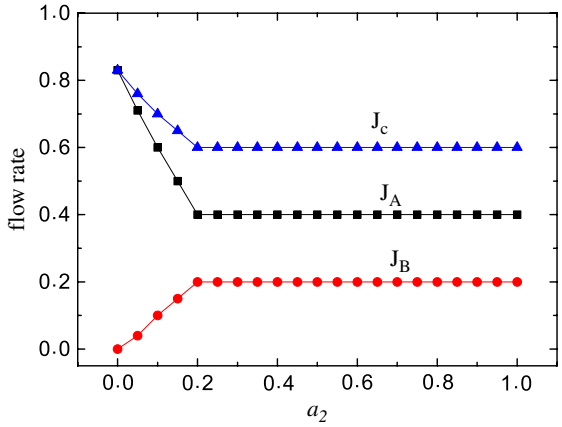

Fig. 3. Dependence of flow rates J_A, J_B and J_C on a_2. The other two injection probabilities are $a_3 = 0$ and $a_1 = 1$.

the evolution of car B_{lead} is affected by car A_{lead}. For cars C_{lead} and D_{lead}, the evolution is the same except that the roles of cars A_{lead} and B_{lead} are replaced by the roles of cars C_{lead} and D_{lead}, respectively.

In our simulation, the same boundary conditions as in Ref. [17] are used. In a single time step, after the evolution of all cars is completed, we check the position of the last car on A (B, D), denoted as A_{last} (B_{last}, D_{last}). If A_{last} (B_{last}, D_{last}) is larger than v_{max}, a car with velocity v_{max} will be injected with probability $a_1(a_2, a_3)$ at the cell $\min[A_{last}(B_{last}, D_{last}) - v_{max}, v_{max}]$. Moreover, if the position of the leading car on road E, denoted as E_{lead}, is larger than L_E (the position of the rightmost cell on road E), it will be removed and its following car becomes the new leading car.

3. The numerical results

In this section, we present and discuss the simulation results. In the simulations, roads A, B, C, D and E are divided into 500 cells unless otherwise mentioned. The system is initially empty and the first 40,000 time steps are discarded to let the transient time die out.

As a preliminary study, Fig. 2 shows the plot of flow rate on the main road versus a_1 in which $a_2 = a_3 = 0$ (i.e., there are no on-ramps); Fig. 3 shows the plot of J_C, the flow rate on road C, versus a_2 in which $a_1 = 1$ and $a_3 = 0$ (i.e., there is only one on-ramp).

From Fig. 2, one can see that, when a_1 is small, the flow rate equals to a_1. When $a_1 > 0.5$, the curve begins to bend down and the flow rate becomes smaller than a_1. When $a_1 = 1$, the flow rate reaches the maximum flow rate 5/6 (in this case, due to our boundary conditions, the distance between two adjacent cars is v_{max}, thus the density on the main road $\rho = 1/(1 + v_{max})$, and as a result the maximum flow rate $J = v_{max} \times \rho = v_{max}/(1 + v_{max}) = 5/6$). Fig. 3 shows that, when $a_2 = 0$, the maximum flow rate 5/6 is reached on road C. For $0 \le a_2 \le 0.2$, the curve of J_C can be approximately described by a linear function, whose slope value is about 7/6:

$$J_C = 5/6 - 7/6 \times a_2. \tag{5}$$

In this range of a_2, road A is in congestion and road B is in free flow. J_E becomes a constant when $a_2 > 0.2$. In this case, both roads A and B are in congestion.

Here we would like to mention that the feature shown in Fig. 3 is important in our work. Our result is robust and model independent, provided this feature could be reproduced in the model. In contrast, if such a feature does not exist in the

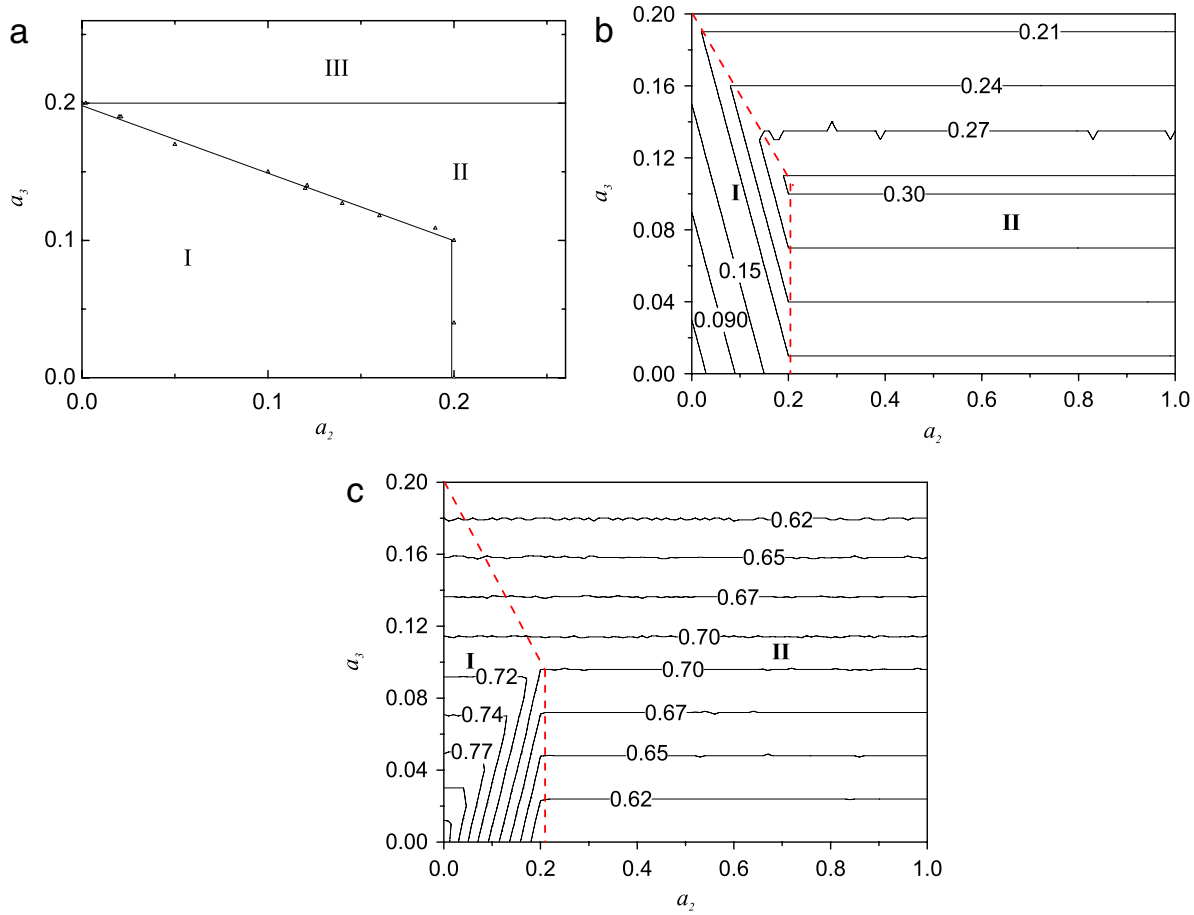

Fig. 4. (a) Phase diagram of the two-on-ramp system, with the parameter $a_1 = 1$. The contour plot in (b) shows the isolines of $J_B + J_D$, and the contour plot in (c) shows the isolines of J_E. The dashed lines represent the boundary between region I and region II.

model (e.g., in the NaSch model with large randomization, in which J_C is independent of a_2; see Ref. [19]), then our result becomes invalid. Fortunately, this feature could be reproduced in most traffic flow models.

Now we present the results when both ramp flows exist. Fig. 4 shows the phase diagram in which $a_1 = 1$. The contour plot in Fig. 4(b) shows the isolines of $J_B + J_D$, and the contour plot in Fig. 4(c) shows the isolines of J_E. One can see that three regions are categorized. Note that road A is congested in regions I–III. The three regions of the phase diagram are discussed below.

Region I: In region I, both roads B and D are in free flow. In this case, the isolines of $J_B + J_D$ are straight lines with slope -1 in the phase diagram. This is due to flow rates on the two ramps being equal to the injection probabilities in this region (i.e., $J_B + J_D = a_2 + a_3$). Now we focus on flow rate J_E obtained on the isolines of $J_B + J_D$, which is shown in Fig. 5. It can be seen that J_E first increases with the increase of J_B. After it reaches the maximum at a critical value $J_{B,c}$, J_E decreases with the further increase of J_B. The critical value $J_{B,c}$ is larger than $(J_B + J_D)/2$, which means that assigning a higher proportion of the demand to the upstream on-ramp could improve the overall flow. This is consistent with previous studies.

Region I is split into two sub-regions (I_1, I_2) by the critical value $J_{B,c}$. Fig. 6(a) and (b) shows the typical spatiotemporal patterns on the main road in the two sub-regions. One can see that, in both regions, road A is congested and road E is in free flow. However, road C is in free flow in region I_2 and is in congestion in region I_1. Fig. 6(c) shows the typical spatiotemporal pattern on road C on the boundary between the two sub-regions, which corresponds to the maximum value of J_E. It can be seen that there exists a shock on road C, and the shock performs a random walk. This kind of shock is typical for a one-dimensional (1D) driven diffusive system at the transition from low density to high density; see, e.g. Ref. [20]. When J_B increases, the flow rate on road C decreases and road C transits into free flow (region I_2). Moreover, J_D decreases since $J_B + J_D$ is fixed. As a result, J_E decreases. On the other hand, if J_B decreases, road C becomes congested (region I_1). Moreover, J_D increases. Consequently, J_E also decreases. This explains why a maximum J_E appears. Next, through an analytical investigation with the help of Eq. (5), we explain why the capacity could be improved by assigning a higher proportion of the demand to the upstream on-ramp.

The flow rate J_E can be calculated in the two sub-regions. In region I_2, the flow rate on road C is (see Eq. (5))

$$J_C = 5/6 - 7/6 \times a_2. \tag{6}$$

Thus,

$$J_E = J_C + J_D = 5/6 - 7/6 \times a_2 + a_3. \tag{7}$$

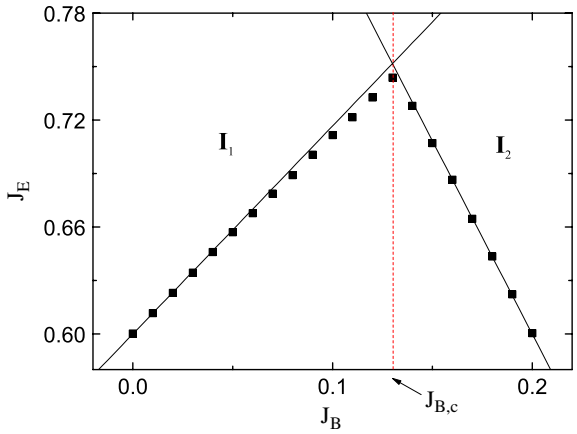

Fig. 5. Dependence of J_E on J_B with fixed J_B+J_D. The parameter $a_1 = 1$, and $J_B+J_D = 0.2$. The solid lines represent the analytical results (see Eqs. (7) and (8)).

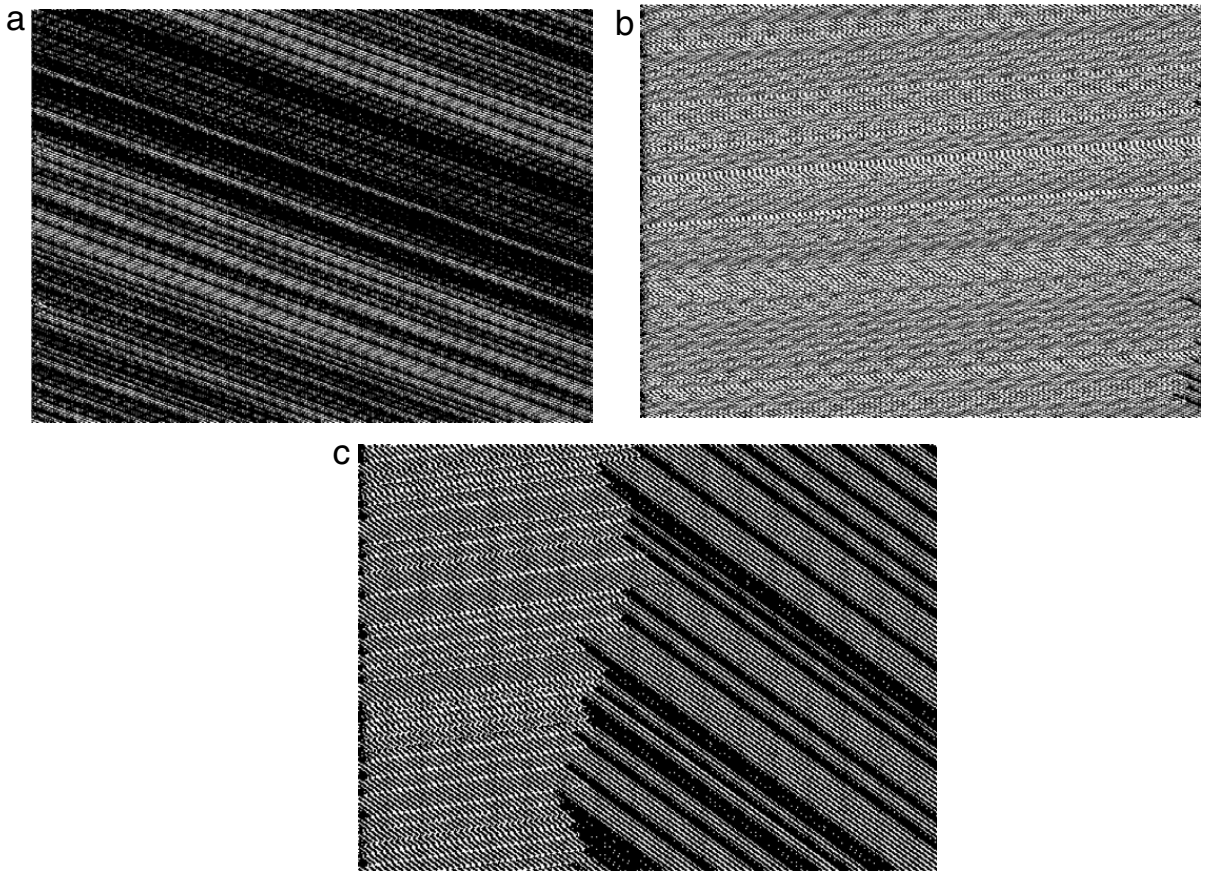

Fig. 6. Typical spatiotemporal patterns on road C (a) in region I_1, (b) in region I_2, (c) at the critical value $J_{B,c}$ (i.e. on the boundary between the two sub-regions). The parameters are $J_0 = 0.1$ and (a) $J_B = 0.03$, (b) $J_B = 0.09$, (c) $J_B = 0.065$. The cars move from left to right and the time increases in the up direction.

In region I_1, it is obvious that (see Eq. (5))

$$J_E = 5/6 - 7/6 \times a_3. \tag{8}$$

Consequently, the maximum flow rate J_E is achieved when

$$5/6 - 7/6 \times a_3 = 5/6 - 7/6 \times a_2 + a_3. \tag{9}$$

Suppose $a_2 + a_3 = J_0$, then (9) becomes

$$5/6 - 7/6 \times J_0 + 7/6 \times a_2 = 5/6 + J_0 - 13/6 \times a_2. \tag{10}$$

The solution is

$$a_2 = 0.65 \times J_0 \tag{11}$$

$$a_3 = 0.35 \times J_0. \tag{12}$$

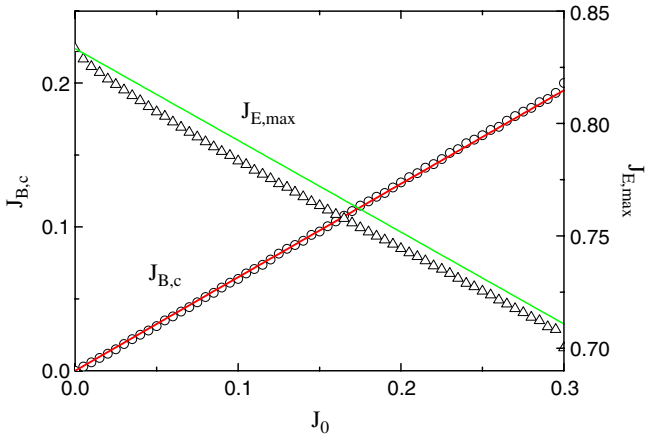

Fig. 7. Dependence of $J_{B,c}$ and $J_{E,\max}$ on J_0. The solid lines are results from Eqs. (13) and (14), and the scattered data are from simulations.

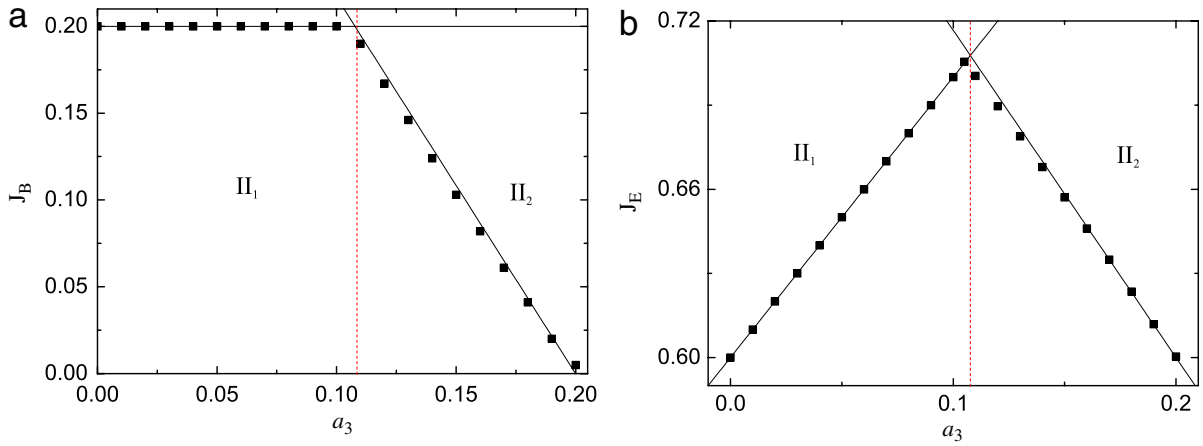

Fig. 8. Dependence of (a) J_B, (b) J_E on a_3. The solid lines are from the analytical investigation. The red dashed lines are boundaries between II_1 and II_2. (For interpretation of the references to colour in this figure legend, the reader is referred to the web version of this article.)

This means that

$$J_{B,c} = 0.65 \times J_0 \tag{13}$$

and

$$J_{E,\max} = 5/6 - 7/6 \times 0.35 \times J_0. \tag{14}$$

The analytical results (7) and (8), also shown in Fig. 5, are in good agreement with the simulations. Fig. 7 shows the dependence of $J_{B,C}$ and $J_{E,\max}$ on J_0. One can see that Eqs. (13) and (14) are also in good agreement with the simulations.

In a general case, Eq. (5) could be expressed as a monotonically decreasing function

$$J_E = f(a_2). \tag{15}$$

In this case, it is easy to derive

$$f(J_{B,c}) - f(J_0 - J_{B,c}) = -J_0 + J_{B,c}. \tag{16}$$

Due to the monotonic decrease of f, it is clear that $J_{B,c} > J_0/2$. This demonstrates that a higher proportion of the demand should be assigned to the upstream on-ramp to improve the overall flow rates.

Region II: In region II, road B has become congested while road D is still in free flow. This region is also split into two sub-regions, as region I. In region II_1, traffic on road C is in free flow. In this case, it is clear that $J_C = 0.6$ and $J_B = 0.2$ (see Fig. 8(a)). Consequently, $J_E = 0.6 + a_3$ (see Fig. 8(b)). The isolines of $J_B + J_D$ become horizontal lines.

In contrast, in region II_2, the traffic on road C becomes congested. As a result, $J_E = 5/6 - 7/6 \times a_3$ (see Fig. 8(b)) and $J_C = 5/6 - 7/6 \times a_3 - a_3$. Since road B is in congestion, J_B is solely determined by J_C and thus solely determined by a_3 (see Fig. 8(a)). An analysis of the traffic flow near cell C_0 shows that $J_B = J_C - 0.4 = 13/30 - 13/6 \times a_3$ (the details are not shown here). Therefore, the isolines of $J_B + J_D$ are still horizontal lines.

The maximum flow rate $J_{E,\max}$ in region II, thus, is achieved when $0.6 + a_3 = 5/6 - 7/6 \times a_3$, which leads to $a_3 = 0.108$ and $J_{E,\max} = 0.708$. The analytical results are in good agreement with simulations (Fig. 8).

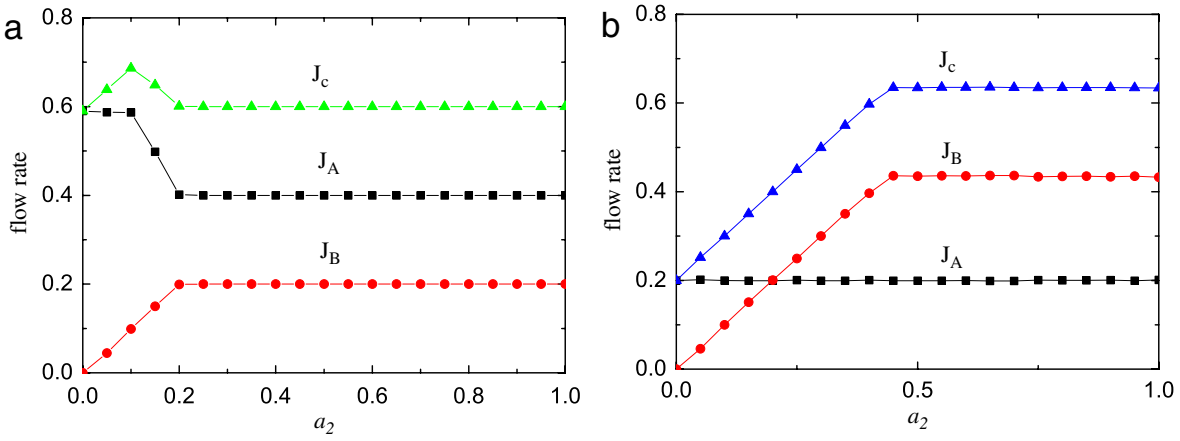

Fig. 9. Dependence of flow rates J_A, J_B and J_C on a_2. The other two injection probabilities are $a_3 = 0$ and (a) $a_1 = 0.6$, (b) $a_1 = 0.2$.

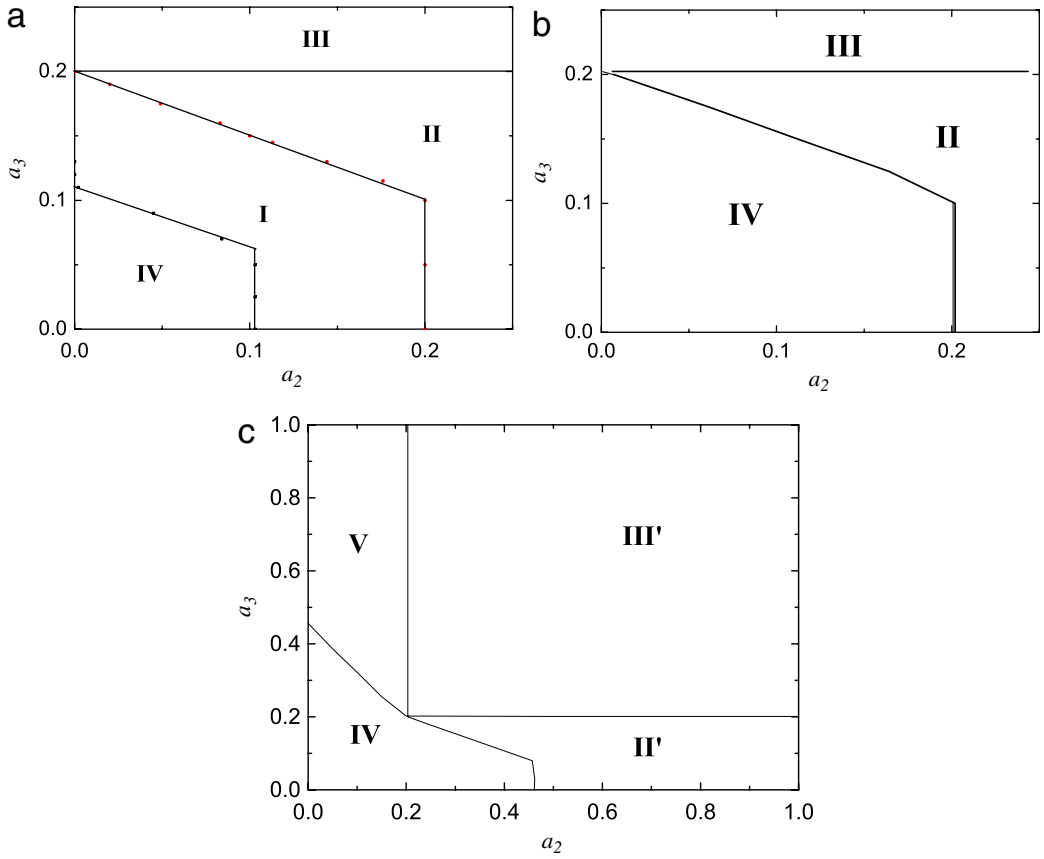

Fig. 10. Phase diagram in which (a) $a_1 = 0.6$, (b) $a_1 = 0.4$, (c) $a_1 = 0.2$.

Region III: In region III both roads B and D become congested. In this case, it is clear that $J_E = 0.6, J_B = 0$ and $J_D = 0.2$. Here $J_B = 0$ is due to the priority rule used in this paper (cf. $J_B = 13/30 - 13/6 \times a_3$ in region II_2).

Next we consider the effect of a_1 on the results. Fig. 9 shows that for one-on-ramp configuration (i.e. $a_3 = 0$), two different situations arise with different range of a_1. Situation 1: When $0.4 < a_1 < 1$, the situation is as shown in Fig. 9(a). With the increase of a_2, J_C first increase from about 0.590, then decrease and finally remains constant at 0.6. Situation 2: When $a_1 < 0.4$, the situation is as shown in Fig. 9(b). With the increase of a_2, J_C first increases from 0.2, and then remains constant at about 0.635.

Fig. 10 shows some typical phase diagrams for $a_1 < 1$. Simulation results show that when $0.4 < a_1 < 1$ (such as $a_1 = 0.6$ in Fig. 10(a)), another region (region IV) appears, in which roads A, B, D are all in free flow. In this region, the isolines of both $J_B + J_D$ and J_E are straight lines with slope -1. This means that J_E only depends on $J_B + J_D$, and no optimal assignment exists.

With the further decrease of a_1, region IV expands, and region I shrinks. When $a_1 = 0.4$, region I disappears (see Fig. 10(b)). Region III remains unchanged.

When $0 < a_1 < 0.4$ (such as $a_1 = 0.2$ in Fig. 10(c)), it can be seen that there are four regions. Regions II′ and III′ appear, which are different from regions II and III only in that road A transits from congested flow to free flow. Another new region (region V) appears, in which roads A and B are in free flow, and road D is in congestion. In region V, the isolines of both $J_B + J_D$ and J_E are vertical lines. When $a_1 = 0$, the phase diagram is the same as Fig. 5 in Ref. [17].

Finally we compare our results with that of Pica Ciamarra. We focus on the case $a_1 = 1$ (Fig. 4(c)) in our work and $P_1 = 1$ (see Fig. 8 in Ref. [15]) in the work of Pica Ciamarra. It can be seen that the results are different. (i) The isolines of J (corresponding to J_E) increase with the increase of P_2 (corresponding to a_2) at the right bottom corner; (ii) When both P_2 and P_3 are small, the isolines of J are essentially straight lines with slope -1. This means that no optimal assignment of on-ramps flow exist. The differences are obviously due to the on-ramp model being unrealistic in that work (see Fig. 4 in Ref. [15], in which the flow rate first increases and then decreases with the increase of P_1 at large maximum velocity; cf. Fig. 3 in this paper).

4. Conclusion

In this paper, we have studied the capacity of a highway with two on-ramps. Although this issue had been investigated before, and it was found that assigning a higher proportion of the demand to the upstream on-ramp could improve the overall flow, the origin of this phenomenon had not been revealed. This paper not only answers why this happens, but also shows under what circumstance it happens. We point out that an optimal assignment exists because the overall flow rate decreases with the on-ramp flow rate, as shown in Fig. 3. While there are altogether seven regions in the 3D space (a_1, a_2, a_3), the optimal assignment is valid only in one of the regions, i.e., both on-ramps are in free flow and the main road upstream of the on-ramps is in congestion. In this region, the optimal assignment is reached when a random walking shock appears on the main road between the two on-ramps. In the other six regions, either the isolines of $J_B + J_D$ are parallel to the isolines of J_E, or J_E is independent of a_2 and a_3. Thus, no optimal assignment exists.

Acknowledgements

The authors acknowledge the support of The National Basic Research Project of China (973 Program No. 2006CB705500), The National Natural Science Foundation of China (Grant Nos. 60744003, 10872149, 10635040, 10532060), and The Specialized Research Fund for The Doctoral Program of Higher Education of China (Grant No. 20060358065).

References

[1] M. Papageorgiou, A. Kotsialos, IEEE Transactions on Intelligent Transportation Systems 3 (2002) 271.
[2] B.S. Kerner, Physica A 355 (2005) 565.
[3] W.P. Xin, P.G. Michalopoulos, J. Hourdakis, D. Lau, Transportation Research Record 1867 (2004) 69.
[4] X.T. Sun, R. Horowitz, Transportation Research Record 1959 (2006) 9.
[5] J.B. Shen, M.S. Chang, IEEE Transactions on Intelligent Transportation Systems 8 (2007) 359.
[6] A. Hegyi, B. De Schutter, H. Hellendoorn, Transportation Research Part C 13 (2005) 185.
[7] L.C. Davis, Physica A 368 (2006) 541.
[8] L.C. Davis, Physica A 361 (2006) 606.
[9] L.C. Davis, Physica A 379 (2007) 274.
[10] R. Jiang, Q.S. Wu, Physica A 366 (2006) 523.
[11] R. Jiang, M.B. Hu, B. Jia, R.L. Wang, Q.S. Wu, Transportmetrica 4 (2008) 51.
[12] H.M. Zhang, W.W. Recker, Transportation Research Part B 33 (1999) 417.
[13] B.S. Kerner, S.L. Klenov, Physical Review E 68 (2003) 036130.
[14] L.C. Davis, Physica A 387 (2008) 6395.
[15] M. Pica Ciamarra, Physical Review E 72 (2005) 066102.
[16] K. Nagel, M. Schreckenberg, Journal of Physics I 2 (1992) 2221.
[17] R. Jiang, Q.S. Wu, B.H. Wang, Physical Review E 66 (2002) 036104.
[18] R. Jiang, Q.S. Wu, B.H. Wang, Physical Review E 67 (2003) 068102.
[19] R. Jiang, B. Jia, Q.S. Wu, Journal of Physics A. Mathematical and General 36 (2003) 11713.
[20] B. Derrida, Physics Reports 301 (1998) 65.